Discrete merging formula

Yu Chen and Sang-Yeun Shim
(Submitted to *Advances in Computational Mathematics*)

August 21, 2002

Abstract. Merging and splitting formulae, essential part of the fast direct solver for the Lippmann-Schwinger equation [1], naturally involve various Green's formulae and thus give rise to singular integrals which are further complicated by the corners of subdomains as a result of subdividing the domain where the scatterer is supported. Therefore to discretize the merging and splitting formulae requires the design of quadrature rules dealing with a range of singularities. The need of quadratures for various singular functions not only strains the effort of discretization but also stresses the efficiency of the fast direct solver because of oversampling required for the quadratures. In this paper we develop necessary numerical tools to overcome these difficulties in discretizing and implementing the fast direct method for the rapid solution of the Lippmann-Schwinger equation in two dimensions.

1 Introduction

In two dimensions, the numerical solution of the Lippmann-Schwinger integral equation for volume scattering is better handled with a direct solver than an iterative one [1], [2], [3]. This is particularly evident for problems with multiple incident waves, and such circumstances arise when we solve the associated inverse scattering problem [4], or when we solve an eigenvalue problem to determine the frequencies of propagating modes in a wave guide.

A fast direct solver for the Lippmann-Schwinger equation relies on the so-called merging and splitting operations [1], [2]. These formulae naturally involve various Green's formulae and thus give rise to singular integrals which are further complicated by the corners of subdomains of the domain where the entire scatterer is supported; therefore to carry out the merging and splitting procedures numerically requires the design of quadrature rules dealing with a range of singularities: Some on the boundary and others in the volume; some related to corners and others not; some associated with the Green's function and others related to its first and second derivatives; some related to the kernel of the integral and others present in the solution of the Lippmann-Schwinger equation; all these and their combinations need to be considered and properly treated in the quadrature rules; see [1] for more details of the singularity types and their combinations.

This need for quadratures for singular functions not only complicates numerical implementation of the merging and splitting operations but also diminishes the efficiency of the fast direct solver, for oversampling and its related processing are necessary for these quadratures.

We present techniques to entire eliminate the difficult quadrature issues in implementing the merging and splitting formulae. This is possible for we choose to first discretize the Lippmann-Schwinger equation, and then perform merging and splitting for the discrete Lippmann-Schwinger equation, instead of directly for the Lippmann-Schwinger equation [1]. In our approach the discrete merging and splitting will be carried out only on the existing mesh points used for discretizing the Lippmann-Schwinger equation, instead of graded mesh required for handling the corner singularities artificially created when subdividing the scatterer.

This approach does not manifest its desirable features without some side effects – the discrete merging and splitting formulae will have fixed accuracies independent of mesh size h. Indeed, they provide only about 4 digit accuracy for the solution of the scattering problem, for a basic version of the discrete merging and splitting formulae. A second version of the discrete formulae, at about 8 times the cost of the basic version, delivers an accuracy of about 8 digits. Versions of higher accuracies are straightforward, but not systematically examined in this paper.

The discrete merging and splitting formulae, as the name indicates, treat the discretized Lippmann-Schwinger equation by regrouping the mesh points into "subscatterers", and organizing them in a hierarchy – objects we need to perform discrete merging and splitting carried out on these discrete subscatterers. How these discrete objects are organized, how we interpret the original, continuous merging and spitting formulae to suit the discrete setting, and how we control accuracy for the discretization comprise the main body of this paper.

The paper is organized as follows. In §2 we define the discrete subdomains and their boundaries. In §3 we establish the approximation properties of the discrete subdomains. We introduce the discrete operators required for the discrete merging and splitting formulae in §4. Finally in §5 we present the discrete merging and splitting formulae.

Remark 1.1 *Due to the technical nature of the merging and splitting formulae, a full development of techniques for their discretization, which is the main task of this paper, will be extremely involved.*

2 Discrete subdomains and their boundaries

In this section, we first discretize the Lippmann-Schwinger integral equation (2) in order to introduce the discrete subdomains in §2.4 and §2.5.

2.1 Lippmann-Schwinger equation

Let q be the scatterer compactly supported in domain $D \subset \mathbb{R}^2$, ϕ_0 be an incident wave, which induces a monopole distribution σ in D that generates the scattered wave ψ

$$\psi = \int_D G(x,\xi)\sigma(\xi). \tag{1}$$

In the forward scattering problem, we solve for σ the Lippmann-Schwinger equation

$$\sigma(x) + k^2 q(x) \int_D G(x,\xi)\sigma(\xi)d\xi = -k^2 q(x)\phi_0(x) \tag{2}$$

2.2 Basic assumptions on D and q

For simplicity in our description of the discrete merging formula, we will assume that the scatterer q is supported in a square domain $D = [0,a] \times [0,a]$ and that it vanishes smoothly over the boundary of D. As is well-known, σ will also vanish smoothly over ∂D, and therefore both can be sampled with high accuracy on a uniform mesh on D

Definition 2.1 *Let $N > 1$ be an integer, $a > 0$ be a real number, and $h = a/(N-2)$. Let D_h be the uniform mesh of N^2 points on the square domain $D = [0,a]^2$, defined by the formula*

$$D_h = \{\, (lh, mh) \,|\, l, m = 0, 1, \cdots, N-1\}. \tag{3}$$

Furthermore, we stipulate to enumerate the N^2 points of D_h from left to right, and from bottom to top (LR-BT); in other words, the points are ordered by

$$(0,0), (h,0), \cdots, (a,0), (0,h), \cdots, (a,h), \cdots (0,a), (h,a), \cdots, (a,a). \tag{4}$$

It is possible to discretize the singular integral (1) to higher orders based on the uniform mesh on D. In fact, such a design exists [5] and is referred to as the corrected trapezoidal quadrature rules. These rules with orders 4, 6, 8, 10, 12, 14, and 20 are available [5].

The assumptions on D and q will simplify the issues of discretization for the Lippmann-Schwinger equation, and make it easier to demonstrate the ideas behind the discrete subdomains. It is possible to develop them for arbitrary domain D where q is compactly supported but does not vanish over the boundary; we will not discuss this issue further in this paper.

2.3 Discretize the Lippmann-Schwinger integral equation

Denote by $G_h \in \mathbb{C}^{N^2 \times N^2}$ the discretized integral operator (1) via a corrected trapezoidal rule [5], by σ_h, q_h, $\phi_{0h} \in \mathbb{C}^{N^2}$ the discretized σ, q, ϕ_0 on the mesh D_h so that

$$\sigma_h = \begin{bmatrix} \sigma_1 \\ \sigma_2 \\ \cdots \\ \sigma_{N^2} \end{bmatrix}, \quad q_h = \begin{bmatrix} q(x_1) \\ q(x_2) \\ \cdots \\ q(x_{N^2}) \end{bmatrix}, \quad \phi_{0h} = \begin{bmatrix} \phi(x_1) \\ \phi(x_2) \\ \cdots \\ \phi(x_{N^2}) \end{bmatrix} \tag{5}$$

and that σ_h is determined with accuracy $O(h^p)$ by solving the algebraic linear equation

$$(I + h^2\, k^2\, q_h\, G_h)\sigma_h = -k^2\, q_h\, \phi_{0h} \tag{6}$$

where the order p can be 4, 6, etc; we will take the fourth order corrected trapezoidal quadrature as an example to illustrate our approach. One of the features of this fourth order rule is that only the correction goes only to the diagonal entries of G_h; therefore, an off-diagonal entry of G_h is simply the Green's function G evaluated at the corresponding source point ξ and field point x; namely,

$$(G_h)_{ij} = G(x_i, x_j), \quad 1 \le i, j \le N^2, \quad x_i, x_j \in D_h \tag{7}$$

Remark 2.2 *For the sixth and higher order rules, the correction goes to some of the off–diagonal entries of G_h. Consequently, these off-diagonal entries will be values of the Green's function G plus correction coefficients imposed by the corrected trapezoidal quadrature. This will complicate our presentation, but will not add any essential difficulties to our approach.*

2.4 A hierarchy of discrete domains

For simplicity, we will assume for the remainder of the paper that there exists positive integer n_1, n_2 such that

$$N = n_1\, 2^{n_2} \tag{8}$$

Definition 2.3 *The set of a square, uniform mesh of points is referred to as a discrete domain.*

Evidently, D_h is a discrete domain. In this section, we will consider discrete domains that are subsets of D_h; we will recursively partition D_h into an n_2 level hierarchy of discrete domains.

First, D_h can be partitioned into four discrete subdomains, as shown in Figure 1. We denote the set of mesh points in each quadrant as follows: The set of grid points in left-bottom box is denoted by D_h^1, the set of mesh points in right-bottom box is denoted by D_h^2, the set of mesh points in right-top box is denoted by D_h^3, and the set of mesh points in left-top box is denoted by D_h^4, i.e.

$$\begin{aligned}
D_h^1 &= \{\, (lh, mh) \,|\, l = 0, 1, \cdots, N/2 - 1,\ m = 0, 1, \cdots, N/2 - 1\} \\
D_h^2 &= \{\, (lh, mh) \,|\, l = N/2 + 1, \cdots, N - 1,\ m = 0, 1, \cdots, N/2 - 1\} \\
D_h^3 &= \{\, (lh, mh) \,|\, l = N/2 + 1, \cdots, N - 1,\ m = N/2 + 1, \cdots, N - 1\} \\
D_h^4 &= \{\, (lh, mh) \,|\, l = 0, 1, \cdots, N/2 - 1,\ m = N/2 + 1, \cdots, N - 1\}
\end{aligned}$$

This procedure of partition can obviously be repeated $n_2 - 1$ times to form the n_2-level hierarchy of discrete subdomains where D_h is said to be on level 0, and D_h^i, $1 \le i \le 4$ are on level 1, and so forth. Each discrete subdomain on a level j with $0 < j < n_2$ is one of the four children of a parent residing on level $j - 1$, and has its own four children residing on level $j + 1$. The discrete subdomains on a level n_2 are referred to as the bottom level subdomains, each having n_1 points of D_h

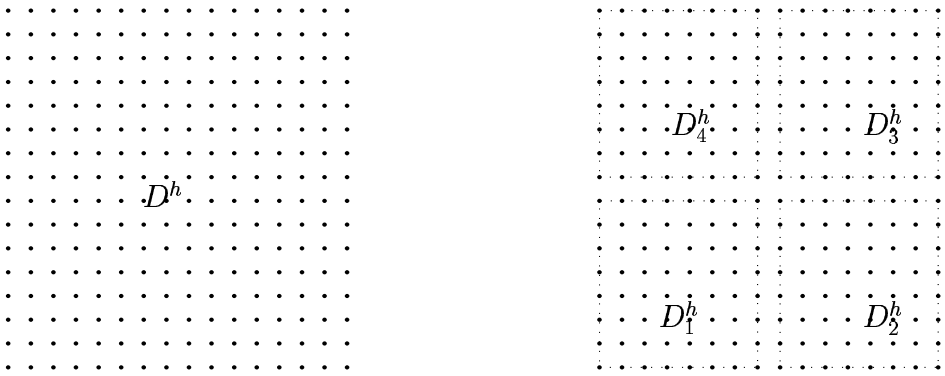

Figure 1: Grouping mesh grid points to construct a hierarchy of discrete subdomains. Left: Mesh points on D_h. Right: D_h divided into its four children.

2.5 Discrete boundaries

A discrete subdomain Ω_h with spacing h can be viewed as layers of points with each layer on a square frame. The set of points on the most outer layer of Ω_h is referred to as the first layer $\mathcal{L}_1(\Omega_h)$; there is of course the second layer $\mathcal{L}_2(\Omega_h)$, and so on. We will denote by $\Gamma_i(\Omega_h)$ or $\Gamma_i(\Omega)$ the square boundary on which the i-th layer lays. The first layer, second layer, etc, putting together, are referred to as the (inner) layers. See Figure 2 for the first layer $\mathcal{L}_1(\Omega_h)$ marked by dots.

Since Ω_h can always be embedded into an infinite, uniform mesh $\mathbb{R}_h^2$ on the plane, the immediate layer outside the first layer, which is not part of Ω_h, is referred to as the first frame $\mathcal{F}_1(\Omega_h)$; there are of course second frame $\mathcal{F}_2(\Omega_h)$, and so forth. We will denote by $\Sigma_i(\Omega_h)$ or $\Sigma_i(\Omega)$ the square boundary on which the i-th frame lays. The first frame, second frame, etc, putting together, are referred to as the (outer) frames. See Figure 2 for the first frames $\mathcal{F}_1(\Omega_h)$ marked by dots.

Remark 2.4 *According to §2.3, an off-diagonal entry of G_h for the fourth order rule is simply the Green's function G evaluated at the corresponding source point ξ and field point x. This means that the discrete monopole charge density σ_h (solution of the discrete Lippman-Schwinger equation (6)) in Ω_h generates the scattered wave*

$$\psi(x) = h^2 \sum_{\xi \in \Omega_h} G(x, \xi)\sigma_h(\xi), \quad x \in \Omega_h \tag{9}$$

We will refer to ψ as the total scattered wave from the discrete subdomain Ω_h for the fourth order rule.

In fact for higher order rules we can consistently define, by incorporating the off-diagonal correction coefficients in (9), the total scattered wave from Ω_h so that the total scattered wave from D_h due to multiple scattering can be obtained as the superposition of these total scattered waves from non-overlapping discrete subdomains whose union is D_h.

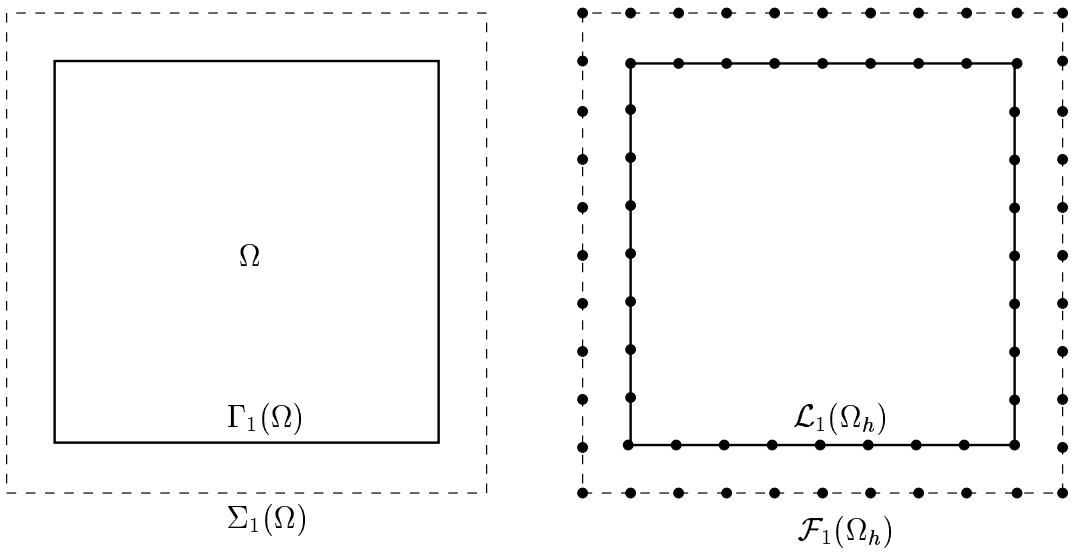

Figure 2: Left: The domain Ω and its boundary $\Gamma_1(\Omega)$ and the square box $\Sigma_1(\Omega)$ enclosing Ω and separated from Ω by h. Right: The first layer $\mathcal{L}_1(\Omega_h)$ and the first frame $\mathcal{F}_1(\Omega_h)$ of Ω_h

Remark 2.5 *The total scattered wave for the discrete subdomain Ω_h is introduced solely for the discrete merging and splitting processes (see §5); it is not required to converge to its continuous counterpart*

$$\psi = \int_\Omega G(x,\xi)\sigma(\xi) \tag{10}$$

as h vanishes. On the other hand, the total scattered wave for D_h, as is well known, will converge to its continuous counterpart (1)

3 Representation of waves by equivalent sources

For the discrete scattering system (6) and (7), an outgoing scattered wave ψ from a discrete subdomain Ω_h of D_h is generated by monopole sources located on mesh points Ω_h (see Remark 2.4), whereas the total incident wave ϕ to Ω_h due to multiple scattering is a superposition of ϕ_0 and all outgoing waves generated by mesh points $D_h \setminus \Omega_h$.

Remark 3.1 *We will assume in the remainder of the paper that the original incident wave ϕ_0 is also generated by monopole sources on points $\mathbb{R}_h^2 \setminus D_h$ (see Remark 3.3 for its justification). We note therefore that the (total) incident wave ϕ to Ω_h is generated by monopole sources located on mesh points $\mathbb{R}_h^2 \setminus \Omega_h$.*

By Green's formula, both the incident (incoming) and scattered (outgoing) waves can be uniquely determined by their boundary data (the Dirichlet and Neumann data) of

the square occupied by Ω_h. In the discrete case, the analog would be to approximate the monopole charges on Ω_h, as sources of outgoing waves, by the monopole charges on the first few layers. Likewise, the monopole charges on mesh points outside Ω_h, as sources of incoming waves, would be approximated by those on the first few frames.

In this section, we investigate numerically the precision of these representations. We will first summarize the main results in Observation 3.2. We will then describe in more details the approximation problems in §3.1. Finally, we will verify the main results numerically in §3.2. Thus the error estimates presented in this section are experimental.

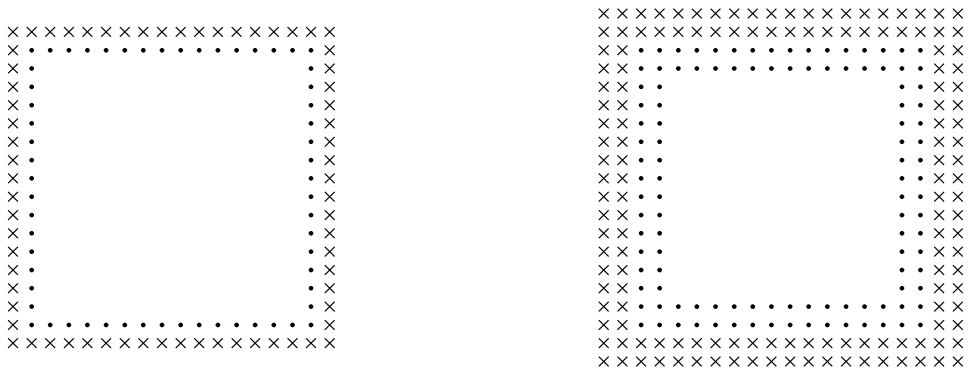

Figure 3: Equivalent monopole charges on the layers are marked by dots, on the frames are marked by 'x'. Left: One layer/one frame is used to allocate equivalent monopole charges for outgoing/incoming waves. Right: Two layers/two frames are used to allocate equivalent monopole charges for outgoing/incoming waves

Observation 3.2 *We discovered numerically that for a sufficiently small $h > 0$ and for any discrete domain Ω_h with at least 8×8 points, any outgoing wave generated by monopole charges on Ω_h and measured at mesh points outside Ω_h can be approximated with the wave generated by an ensemble of equivalent monopole charges on the first layer of Ω_h to about 4 digits provided that k is not an interior Dirichlet eigenvalue; if the first two layers are used, the approximation is about 8 digits. Likewise, any incoming wave generated by the monopole charges on mesh points outside Ω_h and measured on Ω_h can be approximated with the wave generated by an ensemble of equivalent monopole charges on the first frame of Ω_h to about 4 digits; if the first two frames are used, the approximation is about 8 digits. See Figure 3 for the locations of the equivalent monopole charges.*

Better approximation can be obtained when more layers, frames are used. We will not discuss the cases of more than two layers, for 8-digit accuracy is usually sufficient for many applications.

These numerical facts are crucial for our discrete treatment of the scattering matrix and the discrete merging and splitting formulae, in that there is no need to design

sophisticate, less efficient quadrature formulae for singular integrals; there is no need to oversample to overcome singularities at the corners: All boundary-to-boundary linear maps such as the scattering matrices will be discretized on the existing mesh points D_h. See §4.2.

Remark 3.3 *It follows immediately from Observation 3.2 that the assumption made in Remark 3.1 is not a practical constraint on the original incident wave ϕ_0. As long as the actual sources of ϕ_0 are separated from the scatterer D by distance no less than h, ϕ_0 can be approximated by monopole sources on the mesh $\mathbb{R}^2_h \setminus D_h$ with a precision of about 4 digits. If the separation is no less than $2h$, the precision is about 8 digits.*

3.1 The approximation problem

We provide a more precise statement of the mathematical problem for approximation with equivalent sources to the incoming and outgoing waves. For simplicity, we will only describe the single-layer, single-frame cases. The descriptions to be given below can easily be extended to two-layer, two-frame cases.

3.1.1 Approximate incoming waves inside a discrete domain

Since an incoming wave Φ to a discrete domain Ω_h is generated by monopole sources at mesh points outside Ω_h (see Remark 3.1), we have

$$\Phi(x) = \phi_1(x) + \phi(x) \tag{11}$$

where ϕ_1 is due to monopole sources on the first frame, and ϕ is due to the monopole sources at mesh points outside the first frame, and thus can be represented via the Green's formula

$$\phi(x) = \int_{\Sigma_2(\Omega_h)} \left(G(x,\xi)\frac{\partial \phi(\xi)}{\partial n} - \frac{\partial G(x,\xi)}{\partial n(\xi)}\phi(\xi) \right) ds(\xi), \quad x \in \Omega_h \tag{12}$$

To approximate the incoming wave Φ on Ω_h with monopole sources on the first frame $\mathcal{F}_1(\Omega_h)$, therefore, we only need to approximate ϕ on Ω_h with monopole sources on the first frame: Find $\alpha = \{\alpha_j\}$ to solve the least squares problem

$$\sum_{x_j \in \mathcal{F}_1(\Omega_h)} \alpha_j G(x, x_j) = \int_{\Sigma_2(\Omega_h)} \left(G(x,\xi)\frac{\partial \phi(\xi)}{\partial n} - \frac{\partial G(x,\xi)}{\partial n(\xi)}\phi(\xi) \right) ds(\xi), \quad x \in \Omega_h \tag{13}$$

Consequently the incoming wave ϕ is approximated by monopole sources on the first frame

$$\phi(x) = \sum_{x_j \in \mathcal{F}_1(\Omega_h)} \alpha_j G(x, x_j) + \epsilon(x), \quad x \in \Omega_h \tag{14}$$

Introducing

$$\|\phi\|_\star^2 = \int_{\Gamma_1(\Omega_h)} \left[|\phi(x)|^2 + \left| \frac{\partial \phi(x)}{\partial n} \right|^2 \right] ds(x) \tag{15}$$

we refer to

$$E_{rep} = \sup_{\phi} \|\epsilon\|_\star / \|\phi\|_\star \tag{16}$$

as the representation error, which according to Observation 3.2 turns out to be about 10^{-4} for one frame case; see §3.2 for more details. Let's assume that there are some $n \times n$ mesh points on Ω_h.

Remark 3.4 *For efficient computation of α_j, we do not solve (13) with the n^2 points $x \in \Omega_h$; in other words, the incoming wave ϕ is not matched on Ω_h. Instead, we determine α_j to match ϕ and its normal derivative on $\Gamma_1(\Omega_h)$ – the boundary box of Ω_h which is subsequently discretized with some m Legendre points on each of its four sides; see Figure 4. We found that $m = 1.5n$ is sufficient in the sense that further increase in m will not increase the 2-norm of the error term in (13).*

Remark 3.5 *One more discretization is required for numerical solution of (13). We discretize each of the four sides of $\Sigma_2(\Omega_h)$ with about m Legendre points $\{ x_\ell \mid \ell = 1, 2, \ldots, m \}$, with $\{ w_\ell \mid \ell = 1, 2, \ldots, m \}$ being the associated Gaussian weights. Then for each point x_ℓ on $\Sigma_2(\Omega_h)$, we choose the combination $\phi = w_\ell$ and $\partial\phi/\partial n = 0$, and the combination $\phi = 0$ and $\partial\phi/\partial n = w_\ell$, in order to exhaust all possible incoming waves.*

3.1.2 Approximate outgoing wave outside a discrete domain

The approximation problem for the outgoing waves are analogous to that for the incoming waves in §3.1.1, with a major distinction: We must now assume that k is not an interior Dirichlet eigenvalue inside the square boundary $\Gamma_1(\Omega_h)$. If k is, there are outgoing waves that are not representable by single-layer potential on $\Gamma_1(\Omega_h)$, let alone by the discrete monopole charges on $\Gamma_1(\Omega_h)$. This requirement of k is unnecessary when we use the monopole charges on two layers $\mathcal{L}_1(\Omega_h)$, $\mathcal{L}_2(\Omega_h)$ to represent the outgoing waves; see §3.2 and Figure 7 for further details.

Since an outgoing wave Ψ (see (1)) from Ω_h is generated by monopole sources on Ω_h, it assumes the form

$$\Psi(x) = \psi_1(x) + \psi(x) \tag{17}$$

where ψ_1 is due to monopole sources on the first layer $\mathcal{L}_1(\Omega_h)$, and ψ is due to monopole sources on $\Omega_h \setminus \mathcal{L}_1(\Omega_h)$, and thus can be represented via the Green's formula

$$\psi(x) = -\int_{\Gamma_2(\Omega_h)} \left(G(x,\xi) \frac{\partial \psi(\xi)}{\partial n} - \frac{\partial G(x,\xi)}{\partial n(\xi)} \psi(\xi) \right) ds(\xi), \quad x \in \mathbb{R}^2_h \setminus \Omega_h \tag{18}$$

To approximate the outgoing wave Ψ outside Ω_h with monopole sources on the first layer $\mathcal{L}_1(\Omega_h)$, therefore, we only need to approximate ψ by monopole sources on the first layer: Find $\beta = \{\beta_j\}$ to solve the least squares problem

$$\sum_{x_j \in \mathcal{L}_1(\Omega_h)} \beta_j G(x, x_j) = \int_{\Sigma_2(\Omega_h)} \left(G(x,\xi) \frac{\partial \psi(\xi)}{\partial n} - \frac{\partial G(x,\xi)}{\partial n(\xi)} \psi(\xi) \right) ds(\xi), \tag{19}$$

for all $x \in \mathbb{R}^2_h \setminus \Omega_h$. Consequently the outgoing wave is approximated by monopole sources on the first layer

$$\psi(x) = \sum_{x_j \in \mathcal{L}_1(\Omega_h)} \beta_j G(x, x_j) + \varepsilon(x), \quad x \in \mathbb{R}^2_h \setminus \Omega_h. \tag{20}$$

Introducing

$$\|\psi\|^2_* = \int_{\Sigma_1(\Omega_h)} \left[|\psi(x)|^2 + \left| \frac{\partial \psi(x)}{\partial n} \right|^2 \right] ds(x) \tag{21}$$

we refer to

$$E_{rep} = \sup_{\psi} \|\varepsilon\|_* / \|\psi\|_* \tag{22}$$

as the representation error, which according to Observation 3.2 turns out to be about 10^{-4} for one layer case; see §3.2 for more details.

Remark 3.6 *The least squares problem (19) to compute β_j is a standard data fitting one: Find β_j to match ψ at points $x \in \mathbb{R}^2_h \setminus \Omega_h$. For numerical implementation, we avoid these infinite number of points by matching both ψ and its normal derivative on $\Sigma_1(\Omega_h)$ which is subsequently discretized with about m Legendre points on each of its four sides; see Figure 4. See Remark 3.4 for further details on m.*

Remark 3.7 *One more discretization is required for numerical solution of (19). We discretize each of the four sides of $\Gamma_2(\Omega_h)$ with m Legendre points $\{ x_\ell \mid \ell = 1, 2, \ldots, m \}$, with $\{ w_\ell \mid \ell = 1, 2, \ldots, m \}$ being the associated Gaussian weights. Then for each point x_ℓ on $\Gamma_2(\Omega_h)$, we choose the combination $\psi = w_\ell$ and $\partial\psi/\partial n = 0$, and the combination $\psi = 0$ and $\partial\psi/\partial n = w_\ell$, in order to exhaust all possible outgoing waves.*

The extension of §3.1.1 and §3.1.2 to the two layer, two frame case is straightforward, and will not be presented here. For the two layer, two frame case, the corresponding representation errors turn out to be about 8 digits.

3.2 Numerical results

The least squares problem (13), (19) are solved with QR factorization. For a square domain Ω_h, the standard 4-fold symmetry associated with the four sides of the layers and frames can be employed to block diagonalize the matrices for the linear systems (13), (19), and therefore reduces the computational cost. In this section, we present the representation errors of the incoming and outgoing waves described in §3.1.1 and §3.1.2.

3.2.1 Representation errors as a function of h

We measure the representation errors in (13), (19) versus h measured in the number of points per wavelength, n_p. The example given is for a fixed $k = 3$ and for $n_p = 2, \cdots, 20$. Figure 5 shows the relative representation error of the least square problem: using one layer, we get the accuracy of about $O(10^{-4})$ for $n_p \geq 15$. Using two layers, we get the accuracy of about $O(10^{-8})$ for $n_p \geq 15$, for both incoming and outgoing waves.

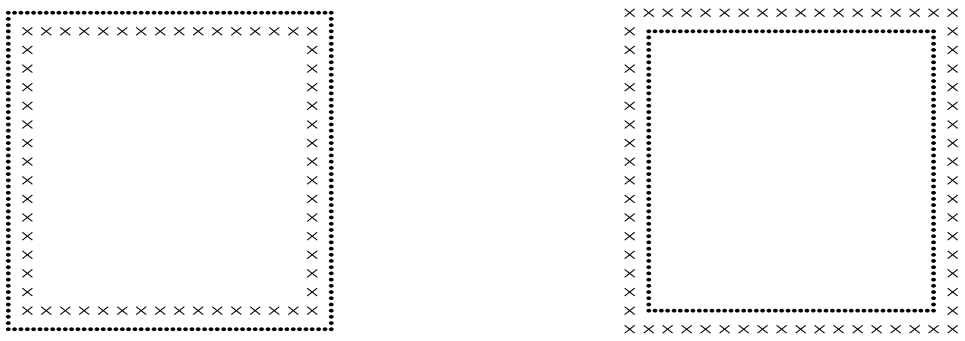

Figure 4: Left: Approximate the outgoing wave ψ with equivalent monopole charges on $\mathcal{L}_1(\Omega_h)$ marked by 'x'. The Legendre points on $\Sigma_1(\Omega_h)$ are marked by dots where ψ and its normal derivative are matched. Right: Approximate the incoming wave ϕ with equivalent monopole charges on $\mathcal{F}_1(\Omega_h)$ marked by 'x'. The Legendre points on $\Gamma_1(\Omega_h)$ are marked by dots where ϕ and its normal derivative are matched.

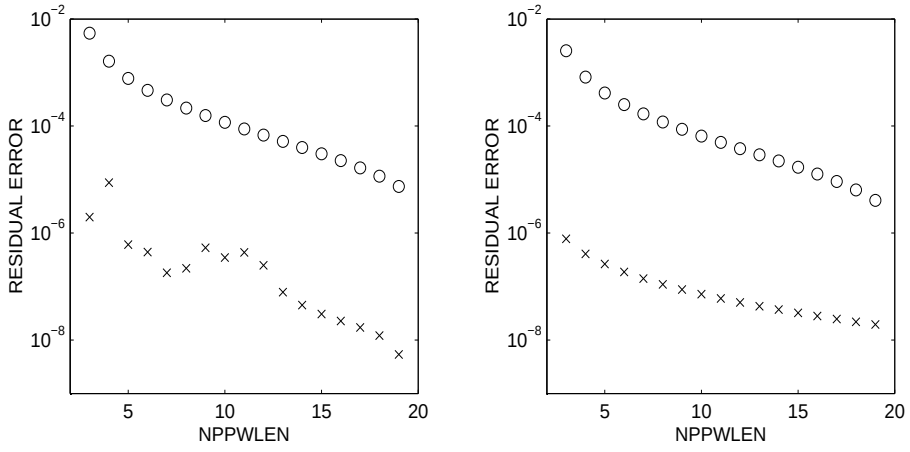

Figure 5: Representation error versus the number of charge points per wavelength (NPPWLEN), at $k = 3$. 'o' for one-layer approximation; 'x' for two-layer approximation. Left: Error for the outgoing waves. Right: Error of incoming waves

3.2.2 Representation errors as a function of k

For fixed $n_p = 15$, and for a range of wave numbers $1 \leq k \leq 25$ with increment $\Delta k = 0.01$, the representation error in (13) for the incoming waves is shown in Figure 6, and the representation error in (19) for the outgoing waves is shown in Figure 7. For the entire range of wave number k, the error for the incoming wave is about $O(10^{-4})$ for one layer, and about $O(10^{-8})$ for two layers. The error for the outgoing wave

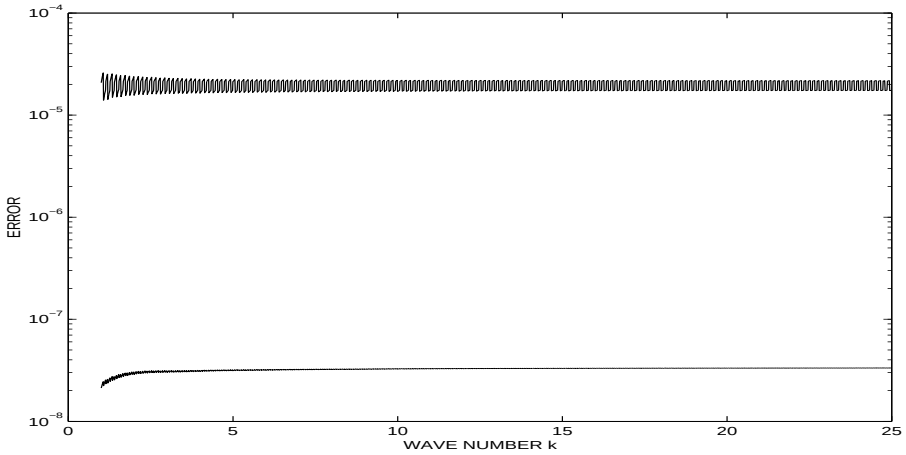

Figure 6: Representation error versus wave number k for the incoming waves. Upper: One-layer approximation. Lower: Two-layer approximation

more erratic due to resonance wave numbers: k being an interior Dirichlet eigenvalues. For non-resonant wave numbers, one layer representation error is about $O(10^{-3})$ away from the interior Dirichlet eigenvalues, and the two layer representation error is about $O(10^{-8})$; see Figure 7.

4 The discrete operators

There are four linear operators required for the merging and splitting formulae of the Lippman-Schwinger equation: The scattering matrix, the restriction, translation, and extension operators; see [1]. In this section, we will introduce their discrete analogs for the discrete merging formula of the discrete Lippman-Schwinger equation (6).

There are two standard ways to define these linear operators (i) Value to value of the wave functions (ii) Coefficients to coefficients of the basis functions representing the wave functions. We will adopt the second approach to treat the Lippman-Schwinger equation. More specifically, we will choose the monopoles as our basis functions, or sources for the incident and scattered waves.

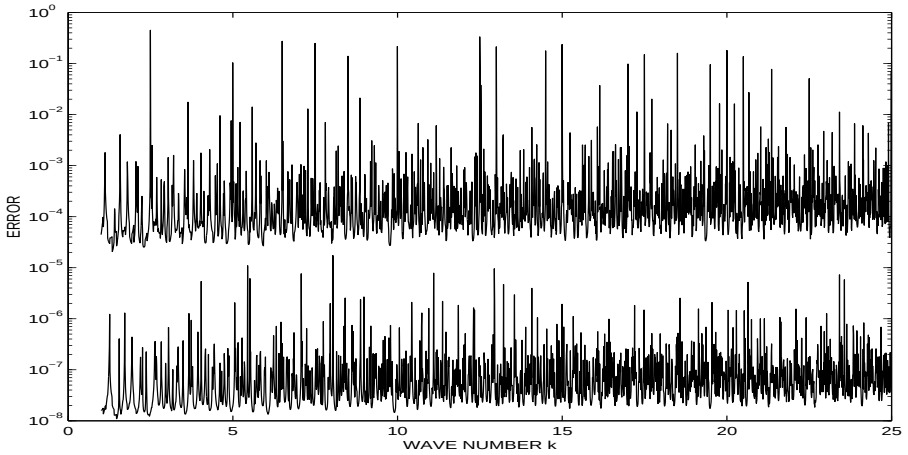

Figure 7: Representation error versus wave number k for the outgoing waves. Upper: One-layer approximation. Lower: Two-layer approximation

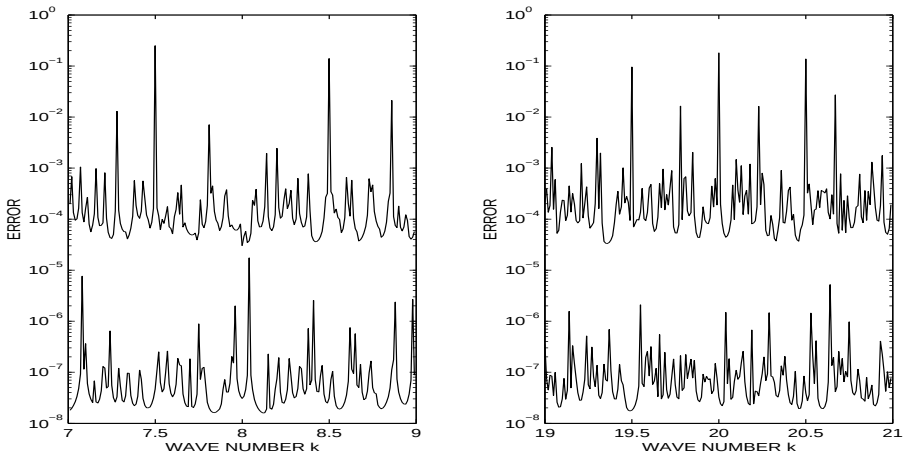

Figure 8: Representation error versus wave number k, zoomed in for the outgoing wave. Left: $7 \leq k \leq 9$. Right: $19 \leq k \leq 21$. Upper: One-layer approximation. Lower: Two-layer approximation

4.1 The scattered wave from a discrete subdomain

Given a discrete subdomain Ω_h, we know that an incident wave ϕ is generated by monopole sources in $x \in \mathbb{R}_h^2 \setminus \Omega_h$. In this section, we wish to define the corresponding scattered wave from Ω_h in order to introduce a discrete scattering matrix for Ω_h in the next section.

Consider the discrete Lippman-Schwinger equation (6) restricted on Ω_h written as

$$P_h \tilde{\sigma}_h = -k^2 \, q_h \, \phi_h \tag{23}$$

where q_h and ϕ_h are q and ϕ restricted on Ω_h; $\tilde{\sigma}_h$ is the solution of this linear algebraic equation which is different from σ_h in (6) even when $\phi = \phi_0$. The corresponding scattered wave from Ω_h, and for the fourth order rule, is defined by the formula

$$\psi(x) = \sum_{\xi \in \Omega_h} G(x, \xi) \tilde{\sigma}_h(\xi). \tag{24}$$

Remark 4.1 *This scattered wave is similar to (9) in that it is a purely algebraic object and not required to converge to any continuous counterpart (see Remark 2.5). It is different from (9), for σ_h in (9) and (6) approximates σ of (1), and is thus physical, whereas $\tilde{\sigma}_h$ in (24) is purely algebraic introduced as a solution to the algebraic equation (23).*

The follow theorem is a direct consequence of (23) and (24), and is crucial for establishing merging and splitting formulae. It's proof is identical verbatim to that of its continuous counterpart [1], and is omitted.

Theorem 4.2 *(***Discrete fundamental law of multiple scattering***) Let Ω_i, $1 \leq i \leq 4$ be the four discrete subdomains of Ω_h as in Figure 9. The total incident wave φ_i to Ω_i is the superposition of the total incident wave ϕ to Ω_h with the scattered waves ψ_j, $j \neq i$ from the other three discrete subdomains. More precisely,*

$$\varphi_i(x) = \phi(x) + \sum_{j \neq i} \psi_j(x), \quad x \in \Omega_i. \tag{25}$$

4.2 The discrete scattering matrix

The scattering matrix for a scatterer D maps the incident wave to the scattered wave, both defined on the boundary of the scatterer [1]. For the discrete domain Ω_h, according to Observation 3.2, the incident wave and scattered wave can be approximated with discrete monopole sources on the frames and layers. We therefore define the discrete scattering matrix S (for the one layer one frame case first) as a matrix mapping the density $\alpha = \{\alpha_j\}$ of monopoles on the first frame $\mathcal{F}_1(\Omega_h)$, which generate the incident wave, to the density $\beta = \{\beta_j\}$ of monopoles on the first layer $\mathcal{L}_1(\Omega_h)$, which generate the scattered wave. More precisely,

$$\beta = S \cdot \alpha \tag{26}$$

where

$$\phi(x) = \sum_{x_j \in \mathcal{F}_1(\Omega_h)} \alpha_j G(x, x_j) + \text{error}, \quad x \in \Omega_h \tag{27}$$

is the incident wave, and

$$\psi(x) = \sum_{x_j \in \mathcal{L}_1(\Omega_h)} \beta_j G(x, x_j) + \text{error}, \quad x \in \mathbb{R}^2_h \setminus \Omega_h. \tag{28}$$

is the scattered wave.

Remark 4.3 *It is obvious to extend the definition of the discrete scattering matrix to the case involving two layers and two frames. As usual, the one layer one frame definition requires that k is not an interior Dirichlet eigenvalue, which is not necessary for the two layer two frame case.*

Remark 4.4 *The discrete operators do not in general converge to their continuous counterparts. These discrete objects are designed purely to improve the efficiency in solving the discretized Lippman-Schwinger equation (6) by discrete merging and splitting processes (see §5).*

4.3 The discrete translation operator

For two disjoint domains Ω_1, Ω_2, an outgoing wave ψ from Ω_1 can be regarded as an incoming wave ϕ to Ω_2. The translation operator T_{21}, for example, maps $\psi|_{\partial\Omega_1}$ to $\phi|_{\partial\Omega_2}$, see [1]. For two disjoint, discrete domains Ω_1, Ω_2 (we have suppressed the subscript h for simplicity), according to Observation 3.2, ψ and ϕ can be approximated with discrete monopole sources on the layers of Ω_1 and frames of Ω_2. We therefore define the discrete translation operator, also denoted by T_{12}, as a matrix mapping the density $\beta = \{\beta_j\}$ of monopoles on the first layer $\mathcal{L}_1(\Omega_1)$, which generate the outgoing wave, to the density $\alpha = \{\alpha_j\}$ of monopoles on the first frame $\mathcal{F}_1(\Omega_2)$, which generate the incoming wave. More precisely,

$$\alpha = T_{21} \cdot \beta \tag{29}$$

where

$$\psi(x) = \sum_{x_j \in \mathcal{L}_1(\Omega_1)} \beta_j G(x, x_j) + \text{error}, \quad x \in \mathbb{R}^2_h \setminus \Omega_1. \tag{30}$$

is the outgoing wave from Ω_1, and

$$\phi(x) = \sum_{x_j \in \mathcal{F}_2(\Omega_2)} \alpha_j G(x, x_j) + \text{error}, \quad x \in \Omega_2 \tag{31}$$

is the incoming wave to Ω_2. See Remark 4.3 for extending the definition to the two layer and two frame case.

4.4 The discrete restriction and extension operators

For two domains Ω and D such that $\Omega \subset D$, an incoming wave ϕ to D is also an incoming wave to Ω. The restriction operator R maps $\phi|_{\partial D}$ to $\phi|_{\partial\Omega}$; see [1]. For two discrete domains $\Omega_h \subset D_h$, according to Observation 3.2, ϕ can be approximated with discrete monopole sources on the frames of D_h and Ω_h. We therefore define the discrete restriction operator, also denoted by R, as a matrix mapping the density $\alpha = \{\alpha_j\}$ of monopoles on the first frame $\mathcal{F}_1(D_h)$, which generate the incoming wave to D_h, to the density $\tilde{\alpha} = \{\tilde{\alpha}_j\}$ of monopoles on the first frame $\mathcal{F}_1(\Omega_h)$, which generate the incoming wave to Ω_h. More precisely,

$$\tilde{\alpha} = R \cdot \alpha \tag{32}$$

where

$$\phi(x) = \sum_{x_j \in \mathcal{F}_1(D_h)} \beta_j G(x, x_j) + \text{error}, \quad x \in D_h \tag{33}$$

is the incoming wave to D_h, and

$$\phi(x) = \sum_{x_j \in \mathcal{F}_1(\Omega_1)} \tilde{\alpha}_j G(x, x_j) + \text{error}, \quad x \in \Omega_h \tag{34}$$

is the incoming wave to Ω_h. See Remark 4.3 for extending the definition to the two layer two frame case.

The definition for the discrete extension operator E is analogous to that for the restriction R. More precisely,

$$\tilde{\beta} = E \cdot \beta \tag{35}$$

where

$$\psi(x) = \sum_{x_j \in \mathcal{L}_1(D_h)} \beta_j G(x, x_j) + \text{error}, \quad x \in \mathbb{R}^2_h \setminus \Omega_h \tag{36}$$

is the outgoing wave from Ω_h, and

$$\psi(x) = \sum_{x_j \in \mathcal{L}_1(\Omega_1)} \tilde{\beta}_j G(x, x_j) + \text{error}, \quad x \in \mathbb{R}^2_h \setminus D_h \tag{37}$$

is the outgoing wave to D_h. See Remark 4.3 for extending the definition to the two layer two frame case.

4.5 Compute the discrete operators

Except the scattering matrix S, all the other three types of discrete operators R, E, and T_{ij} depend only on the geometry of the discrete subdomains involved, and thus can be precomputed. We will take T_{21} as an example to illustrate their computation for the case of four children merged to a parent in which T_{21} is required; see Figure 9.

Let $\gamma_0 = \mathcal{L}_1(\Omega_1) \cap \mathcal{F}_1(\Omega_2)$, $\gamma_1 = \mathcal{L}_1(\Omega_1) \setminus \gamma_0$, and $\gamma_2 = \mathcal{F}_1(\Omega_2) \setminus \gamma_0$. It follows directly from (29) that T_{21} can be partitioned into the 2-by-2 blocks

$$\begin{bmatrix} \tau_{00} & \tau_{01} \\ \tau_{20} & \tau_{21} \end{bmatrix} \tag{38}$$

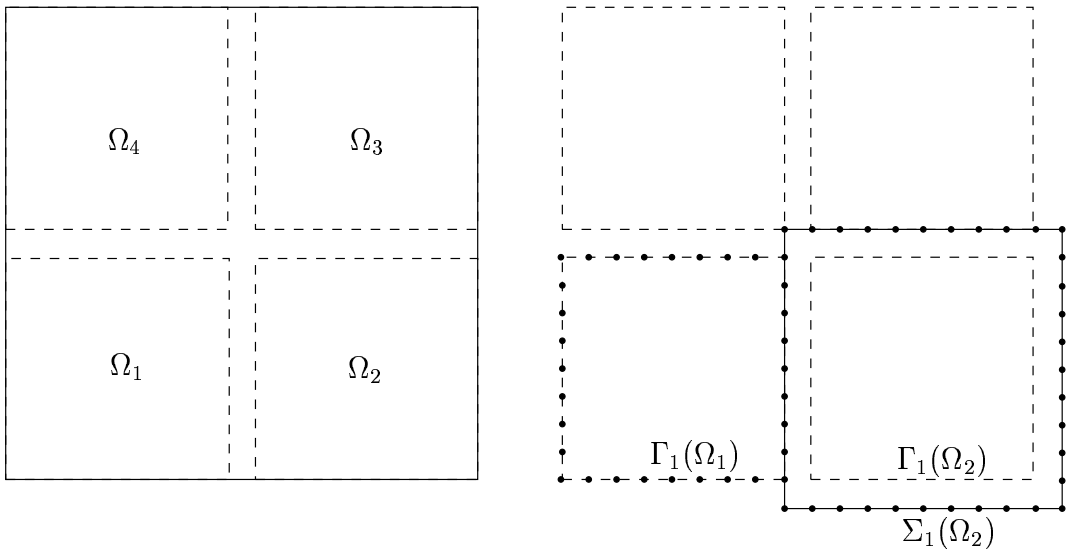

Figure 9: Left: The four discrete subdomains Ω_i, $1 \le i \le 4$ in their parent domain Ω_h. Right: Geometry for the translation operator T_{21}. The subdomains are separated by h; therefore a portion of $\Gamma_1(\Omega_1)$ overlaps with $\Sigma_1(\Omega_2)$

Since T_{21} maps the monopole charge density on $\mathcal{L}_1(\Omega_1)$ to that on $\mathcal{F}_1(\Omega_2)$ so that both represent the same wave in Ω_2 as the incoming wave, we obtain immediately

$$\tau_{00} = I, \quad \tau_{20} = 0 \tag{39}$$

We now determine the two blocks in the second column of (38): Let

$$t_{21} = \begin{bmatrix} \tau_{01} \\ \tau_{21} \end{bmatrix}, \quad \text{with} \quad \alpha = t_{21} \cdot \beta|_{\gamma_1} \tag{40}$$

It follows from (13) immediately that we are required to solve for t_{21} the least squares problem

$$\sum_{x_j \in \mathcal{F}_1(\Omega_2)} (t_{21} \cdot \beta|_{\gamma_1})_j G(x, x_j) = \sum_{\xi_j \in \gamma_1} (\beta|_{\gamma_1})_j G(x, \xi_j), \quad x \in \Omega_2 \tag{41}$$

namely, to match the incoming wave on Ω_2 generated by $\beta|_{\gamma_1}$ with that by α. According to Remark 3.4, (41) will be solved not at $x \in \Omega_2$, but at m Legendre points, here denoted by ℓ_m on $\Gamma_1(\Omega_2)$. Letting p be the number of points on $\mathcal{F}_1(\Omega_2)$, q be the number of points on γ_1, and ν be the inward normal on $\mathcal{L}_1(\Omega_2)$ we therefore define the $2m$-by-p matrix A via the formula

$$(A \cdot \alpha)(x) =: \begin{bmatrix} \sum_{x_j \in \mathcal{F}_1(\Omega_2)} G(x, x_j)\alpha_j \\ \sum_{x_j \in \mathcal{F}_1(\Omega_2)} \frac{\partial G(x, x_j)}{\partial \nu(x)} \alpha_j \end{bmatrix}, \quad x \in \mathcal{L}_1(\Omega_2) \tag{42}$$

so that

$$\begin{bmatrix} \phi \\ \frac{\partial \phi}{\partial \nu} \end{bmatrix}_{\mathcal{L}_1(\Omega_2)} = A \cdot \alpha \tag{43}$$

is the incoming wave and its normal derivative due to monopole sources α on $\mathcal{L}_1(\Omega_2)$. Similarly, we define the $2m$-by-q matrix B via the formula

$$(B \cdot \beta)(x) =: \begin{bmatrix} \sum_{x_j \in \gamma_1} G(x, x_j)\beta_j \\ \sum_{x_j \in \gamma_1} \frac{\partial G(x,x_j)}{\partial \nu(x)}\beta_j \end{bmatrix}, \quad x \in \mathcal{L}_1(\Omega_2) \tag{44}$$

so that

$$\begin{bmatrix} \phi \\ \frac{\partial \phi}{\partial \nu} \end{bmatrix}_{\mathcal{L}_1(\Omega_2)} = B \cdot \beta \tag{45}$$

is the incoming wave and its normal derivative due to monopole sources β on γ_1. Then the arbitrariness of $\beta|_{\gamma_1}$ reduces (41) to

$$A \cdot t_{21} = B \tag{46}$$

whose least squares solution for t_{21} can be obtained by standard SVD on A with suitable regularization by cutting off the smaller singular values.

Remark 4.5 *This computation for T_{21} via t_{21} can obviously and easily be extended to the two layer two frame case. For the one layer one frame case, we recommend the spectral cutoff at 10^{-4} for regularization of (46), and the corresponding relative residual for (46) is about 10^{-4}, as expected and consistent with the level of error in (14). For the two layer two frame case, the spectral cutoff is 10^{-8}, and the relative residual is about 10^{-8}.*

5 The discrete merging and splitting formulae

In this section we will first establish procedures for computing the discrete scattering matrix for a discrete subdomain Ω_h via the solution of the discrete Lippman-Schwinger equation (6). We will then present the discrete merging and splitting formulae which are also used to compute the discrete scattering matrix via merging the scattering matrices for the child subdomains of Ω_h. The use of the discrete merging and splitting formulae for the rapid solution of the discrete Lipmann-Schwinger equation (6) is identical to its continuous counterpart [1], and will not be described in this paper.

We have so far established in the three preceding sections all essential analytical machinery for the discrete merging and splitting formulae, which turn out to be identical in algebraic form to their continuous counterpart.

5.1 Directly compute the discrete scattering matrix

Let there be $r = n^2$ mesh points in Ω_h. Then there are $p = 4(n-1)$ points on the first layer $\mathcal{L}_1(\Omega_h)$, $q = 4(n+1)$ points on the first frame $\mathcal{F}_1(\Omega_h)$. The r-by-q matrix G_{vb} defined by the formula

$$(G_{vb} \cdot \alpha)(x) = \sum_{x_j \in \mathcal{F}_1(\Omega_h)} G(x, x_j)\alpha_j, \quad x \in \Omega_h \tag{47}$$

maps monopole charges α on $\mathcal{F}_1(\Omega_h)$ to incident wave $\phi(x) = (G_{vb} \cdot \alpha)(x)$ on Ω_h. The p-by-r matrix G_{bv} defined by the formula

$$(G_{bv} \cdot \tilde{\eta})(x) = \sum_{x_j \in \Omega_h} G(x, x_j)\tilde{\eta}_j, \quad x \in \mathcal{L}_1(\Omega_h) \tag{48}$$

maps monopole charges η on Ω_h to the scattered wave $\phi(x) = (G_{vb} \cdot \alpha)(x)$ on $\mathcal{L}_1(\Omega_h)$. It follows immediately from (26) and (23) that

$$S = -k^2\, G_{bv} \cdot P_h^{-1} \cdot q_h \cdot G_{vb} \tag{49}$$

The formula is useful in computing the scattering matrix for a small discrete subdomain Ω_h which in practice contains usually no more than 10-by-10 grid. Scattering matrix for large discrete subdomains are obtained more efficiently by merging; see §5.

The above definitions and formulae can be extended easily to the two layer two frame case.

5.2 Discrete merging and splitting formulae

In this section, we present the discrete merging and splitting formulae directly implementable for the rapid solution of the discrete Lippman-Schwinger equation (6))

Let $S_i,\ 1 \le i \le 4$ be the discrete scattering matrices for the discrete subdomains $\Omega_i\ 1 \le i \le 4$ whose parent is Ω_h; see Figure 9. Let $R_i,\ E_i,\ 1 \le i \le 4$ be the restriction and extension matrices, and let $T_{ij},\ 1 \le i, j \le 4; i \ne j$ be the translation matrices.

Denote by S_p the discrete splitting operator defined by the formula

$$S_p = \begin{bmatrix} I & -T_{12}S_2 & -T_{13}S_3 & -T_{14}S_4 \\ -T_{21}S_1 & I & -T_{23}S_3 & -T_{24}S_4 \\ -T_{31}S_1 & -T_{32}S_2 & I & -T_{34}S_4 \\ -T_{41}S_1 & -T_{42}S_2 & -T_{43}S_3 & I \end{bmatrix}^{-1} \begin{bmatrix} R_1 \\ R_2 \\ R_3 \\ R_4 \end{bmatrix} \tag{50}$$

The merging and splitting formulae are not exact due to errors in the representations (14), for the incident, and (20), for the scattered waves.

Theorem 5.1 *(***Discrete merging formula***) Upto the representation errors, the scattering matrix S for Ω_h can be obtained from $S_i,\ 1 \le i \le 4$ of its four children via the merging formula*

$$S = [E_1\, E_2\, E_3\, E_4] \cdot S_p \tag{51}$$

The proof is based on Theorem 4.2, and is identical verbatim to that of its continuous counterpart [1], and is omitted.

Theorem 5.2 *(***Discrete splitting formula***) Upto the representation errors, the total incident waves φ_i to Ω_i, for $1 \le i \le 4$ can be obtained from the total incident wave ϕ to Ω_h via the splitting formula*

$$\begin{bmatrix} \varphi_1 \\ \varphi_2 \\ \varphi_3 \\ \varphi_4 \end{bmatrix} = S_p \cdot \phi \tag{52}$$

The proof is identical verbatim to that of its continuous counterpart [1], and is omitted.

References

[1] Y. Chen, *A fast, direct algorithm for the Lippmann-Schwinger integral equation in two dimensions*, *Advances in Computational Mathematics*, vol. 16, pp. 175-190, 2002

[2] J. Ma, V. Rokhlin, and P. Jones (1994) *A Fast Direct Algorithm for the Solution of the Laplace Equation on Regions with Fractal Boundaries, Journal of Computational Physics*, Vol 113, No. 1, July 1994.

[3] W. Chew, C. Lu *The use of the Huygens' equivalence principle for solving the volume integral equations of scattering,* IEEE ANTENNAS PROPAG vol. AP-41, no. 7, pp. 897-904, July 1993

[4] S. Y. Shim and Y. Chen *Recursive Sherman-Morrison Factorization for Scattering Calculations*, submitted to *Inverse Problems*

[5] J. C. Aguilar and Y. Chen (2002) *High order corrected trapezoidal quadrature rules for functions with a logarithmic singularity in 2-D*, Computers & Mathematics with Applications